

# Equilibria of diffusive moist static energy balance model

Yutian Wu

January 12, 2009

## Introduction

Temperature is a key variable in the measurement of climate. The first order approximation of temperature can be derived from the global energy balance model. The basic idea of the global energy balance of the Earth is that the incoming solar radiation should always keep in balance with the energy back to space by Earth's radiative emission. Because of the transparency of the Earth's atmosphere to the incoming solar radiation and the opaque characteristics to the terrestrial radiation, the absorption of solar radiation mostly takes place at the surface while most of the emission happens at top of the atmosphere. Budyko (1969)[4] and Sellers (1969)[11] brought up a type of energy balance model by using the zonal and annual averaging but allowing the latitudinal dependences of surface temperature, albedo and meridional heat transport. One of the major features of this type of model is that it presented the possibility of an abrupt transition to a completely ice-covered Earth if the solar constant is lowered by only a few percent.

My project aims to figure out the effect of water vapor in this type of energy balance model. The effect of water vapor is significant on climate but complicated to analyze. First of all, water vapor is one of the most important greenhouse gases of the atmosphere and has a positive feedback on climate change: if anything happens to initiate a small temperature increase of the atmosphere, due to the saturation vapor pressure given in Clausius-Clapeyron equation, more water vapor can be held in the atmosphere. The additional water vapor will lead to additional greenhouse effect which warms the Earth further beyond the initial warming. Intergovernmental Panel on Climate Change (IPCC) Fourth Assessment Report (AR4)[7] suggested that water vapor changes represent the largest positive feedback affecting equilibrium climate sensitivity, and it is this key positive feedback that amplifies the response to the anthropogenic forcing. In addition, water vapor is playing a major role in determining the atmospheric convection and cloud cover, which in turn exerts complicated feedback on climate. However, cloud feedbacks still remain the largest source of uncertainty in the projection of climate change. Finally water vapor is an important component in atmospheric circulation and hydrological cycles. With increased moisture in the atmosphere in the future climate baroclinic eddies may increase in strength, on the other hand, the temperature gradient from the equator to the poles may decrease due to the increased poleward moisture energy transport. Because of the many aspects of the impacts of water vapor on the climate and various complicated water vapor feedbacks, the net effect of water

vapor is complicated to analyze in real climate. In this study, we develop simple numerical models with parameterizations of basic but essential physics. Rather than full-blown General Circulation Models, simplified models can be understood completely and may be able to address big questions in real climate. Section 1 introduces an one-layer diffusive moist static energy balance model. Rather than sensible heat merely, moist static energy is applied which includes not only sensible heat but also latent heat and potential energy. Although the one-layer model has represented several interesting features, it cannot produce modern climate even though all the model parameters are of modern values; in addition, not much water vapor effect can be realized except the substantial atmospheric moisture transport to the poles. The reason for it might be the one-layer model itself is too simple to represent the real situation of the climate, for example clouds, which is an important component of climate associated sensitively with water vapor in the atmosphere. Clouds have substantial interactions with both solar and terrestrial radiation in both radiation reflection and absorption, therefore a net energy loss or gain to the atmosphere-Earth system can be produced by clouds depending on their characteristics. Although the net nonradiative and radiative effect of clouds is hard to predict, clouds do have the potential for climate change. Lots of study has been focused on the physics of clouds and narrowing down the uncertainty of cloud-climate feedback in model simulations. In Section 2 a simple two-layer atmosphere-surface model is developed to implement the most basic but essential physics of one of the most important features of water vapor, i.e. cloud feedback. In the discussion we apply the basic idea of convective cloud feedback which was first proposed by Abbot and Tziperman (2007)[2] to explain the equable climate during the late Cretaceous and early Paleogene (about 100 million to 35 million years ago). Geological data suggests that the Earth was much warmer than it is today, especially at high latitudes and during winter time. For example, there were palm trees in Wyoming and crocodiles on islands in the Arctic ocean. The equator to pole temperature difference and the amplitude of the seasonal cycle at high latitudes were relatively small, hence the name "equable climate". The basic idea of convective cloud feedback is that an initial warming, for example, due to the increase of  $CO_2$  concentration, leads to the moist destabilization of the high-latitude atmosphere and initiates atmospheric convection. The resulting convective clouds and atmospheric moisture both help trap the outgoing longwave radiation, leading to further warming. Furthermore since convective cloud feedback allows for multiple equilibria[2], more equilibria are expected in the two-layer model when compared with the equilibria in the one-layer one. The physics of those equilibria is also interesting to know, which is demonstrated in Section 3. In Section 4, a seasonal model is set up when both the time-varying solar insolation and cloud albedo effect are taken into account, for example, more solar incoming radiation is reflected when convection happens due to the cloud albedo effect. We also explore the numerical time-dependent solutions of the seasonal model.

## One-layer Model

A one-layer model is set up based on the Budyko-Sellers type of energy balance model, in which the basic idea of global energy balance is applied and the energy transport is diffusive.

The model is defined by [8][9][5]

$$C \frac{\partial T}{\partial t} = \frac{\tilde{D}}{a^2 \cos(\phi)} \frac{\partial}{\partial \phi} [\cos(\phi) \frac{\partial M}{\partial \phi}] + S - OLR \quad (1)$$

where  $C$  is the thermal inertia,  $T$  is the temperature and  $\tilde{D}$  is the diffusion coefficient.  $a$  is the Earth radius,  $\phi$  is the latitude.  $M$  is the moist static energy which is defined as  $M = C_p T + Lq + gz$ , where  $C_p$  is the specific heat capacity at constant pressure,  $L$  is the latent heat release,  $q$  is the specific humidity and  $z$  is the height of the parcel.  $S$  is the incoming solar radiation which is given by

$$S = L_{\odot}(1 - \alpha)F(\phi) \quad (2)$$

where  $L_{\odot} = 1370W/m^2$  is the solar constant.  $\alpha$  is the albedo. Albedo is not a static quantity, however, is determined sensitively by the processes in the atmosphere and at the surface. As climate changes, the surface characteristics change, for example, the proportion of the Earth's surface covered by ocean water, sea ice, land ice, vegetation and so on, and the resulting albedo changes feed back on the state of the climate. In this model I choose a simple but reasonable representation of albedo which is given by

$$\alpha(T) = \begin{cases} \alpha_i & \text{for } T \leq T_i \\ \alpha_o + (\alpha_i - \alpha_o) \frac{(T - T_o)^2}{(T_i - T_o)^2} & \text{for } T_i < T < T_o \\ \alpha_o & \text{for } T \geq T_o \end{cases} \quad (3)$$

where  $\alpha_i$  and  $\alpha_o$  are albedos of sea ice and ocean water, respectively, and  $T_i$  and  $T_o$  are two threshold temperatures. When surface temperature is very large within some area, i.e.  $T_s > T_o$ , it is above freezing and there is no ice, thus in this case, the albedo is given by the ocean water albedo; when surface temperature is very low, i.e.  $T_s < T_i$ , it is completely covered by sea ice thus the albedo is given by the sea ice albedo within some area. In between it is reasonable to interpolate the albedo by a quadratic form given above.  $F$  is the annual mean flux factor of solar incoming radiation, which gives the latitudinal distribution of solar flux. It peaks at the equator and decreases gradually to the poles.  $OLR$  is the outgoing longwave radiation which is a function of the emission temperature  $T_e$  at top of the atmosphere, i.e.  $OLR(T_e) = \sigma T_e^4$ , where  $\sigma$  is the Stefan-Boltzmann constant. Budyko (1969)[4] applied a linearized version of  $OLR$ , based on the fact that  $T_e$  is linearly related to the surface temperature  $T_s$ , which is given by

$$OLR(T_e) \approx A + BT_s \quad (4)$$

where  $A$  and  $B$  are constants that can be deduced from the fitting of observations.  $A$  is roughly linear in  $1/\log(CO_2)$  concentration. By analyzing the data of monthly mean upward longwave radiation flux and surface air temperature from year 1961 to 2000 in NCEP/NCAR Reanalysis Data,  $A = 211.2W/m^2$  and  $B = 2.09W/m^2(^{\circ}C)^{-1}$  produces the best fit between the annual mean fluxes calculated using the linearized approximation and the reanalysis data.

By defining variable  $y = \sin(\phi)$ , the equation of steady-state solution can be rewritten as

$$\frac{\tilde{D}}{a^2} \frac{d}{dy} [(1 - y^2) \frac{dM}{dy}] = OLR(T_s(y)) - S(y). \quad (5)$$

Steady-state solutions are important because a Lyapunov functional has been found in the previous PDE which implies all time-dependent solutions will eventually converge to stable steady-state solutions just like the case in Budyko-Sellers type of energy balance model. Because it is symmetric between the Northern and Southern Hemisphere in the model, only northern hemisphere is discussed here, i.e.  $0 \leq y \leq 1$ . For boundary conditions, take  $\frac{dT}{dy} = 0$  at the equator, which enforces symmetry between the two hemispheres, and insist that  $T$  be regular at the poles.

Since  $M$  is conserved under conditions of either dry adiabatic ascent (exactly) or saturated adiabatic ascent (approximately),  $M$  can be expressed in the term of  $T_s$  based on the surface moist static energy and Clausius-Clapeyron equation, i.e.

$$M = C_p T + Lq + gz \quad (6)$$

$$= C_p T_s + L_v q_s \quad (7)$$

$$= C_p T_s + h_s L_v q_s^* \quad (8)$$

$$= C_p T_s + h_s L_v \frac{R_d}{R_v} \frac{1}{p_s} e_s^* \quad (9)$$

$$= C_p T_s + h_s L_v \frac{R_d}{R_v} \frac{1}{p_s} e_s(T_o) \exp\left[\frac{L_v}{R_v} \left(\frac{1}{T_o} - \frac{1}{T_s}\right)\right] \quad (10)$$

where the subscripts  $s$  represent surface values, the superscripts  $*$  represent saturation values.  $L_v$  is the latent heat release of evaporation,  $h_s$  is the surface relative humidity which is assumed to be a constant everywhere,  $q_s^*$  is the saturation specific humidity at the surface,  $T_o = 273.15K$ ,  $R_d$  and  $R_v$  are the gas constants for dry air and water vapor, respectively,  $p_s$  is the surface pressure, and  $e_s(T_o) = 6.11mb$  is the saturation vapor pressure at  $T_o$ .

Now the climate is characterized by the annual average and global mean surface temperature  $T_s$ , and the steady-state equation becomes an nonlinear ODE of  $T_s$  which can be solved numerically. For fixed  $A$  and  $B$  (fixed  $CO_2$  concentration and thus fixed  $OLR$  in this model), for example,  $A = 211.2W/m^2$  and  $B = 2.09W/m^2(^{\circ}C)^{-1}$  which are the parameters derived from fitting the current climate data, but for different initial guesses, steady-state solutions are not always the same, which implies the existence of bifurcation. Hence instead I solve  $A$  (for fixed  $B$ ) as an unknown parameter by prescribing the equatorial surface temperature  $T_s(y = 0)$ . Figure 1 shows the steady-state solutions of this model as a function of  $A$ . In particular, not only equatorial surface temperature  $T_s(y = 0)$  but also polar surface temperature  $T_s(y = 1)$  and mean surface temperature are drawn. The bifurcation diagram is composed of a stable ice-free climate  $a$ , an unstable climate  $b$  and a stable snowball climate  $c$ . In particular, for  $A = 211.2W/m^2$ , three possible climate states are shown in Figure 2. They are a stable snowball climate where temperature is below freezing everywhere on the Earth, an unstable climate which is  $20K$  lower than the current climate everywhere from the equator to the poles, and a stable ice-free climate where temperature is relatively high everywhere and the temperature difference between the equator and poles is relatively small, respectively. As for the unstable climate, although it is  $20K$  lower than the current climate, the temperature gradient from the equator to the poles which is about  $40K$  is quite reasonable. In addition, a comparison of the steady-state solutions has been done between the dry (Figure 3) and moist diffusive energy balance model. For the dry

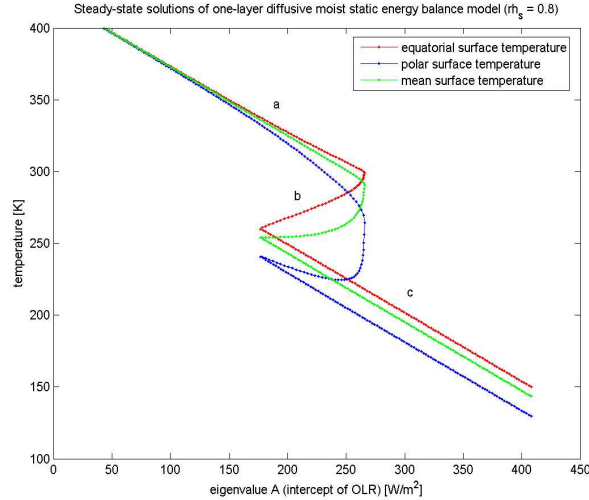


Figure 1: Steady-state solutions of one-layer diffusive moist static energy balance model as a function of  $A$ , which is roughly linear in  $1/\log(CO_2)$  concentration. Relative humidity is assumed to be 0.8 everywhere. Model parameters are:  $\alpha_i = 0.6, \alpha_o = 0.1, T_i = 260K, T_o = 290K, B = 2.09W/m^2(^{\circ}C)^{-1}$ .

diffusive energy balance model, there is no latent heat in the energy term but only sensible heat. The major difference between the steady-state solutions of the two models is that for the ice-free climate the temperature gradient from the equator to the poles is relatively small in the moist case while it is roughly  $50K$  in the dry one. My explanation for such a difference is that in hot climate water vapor helps transport large amount of energy poleward effectively and thus wipes out the temperature gradient. This is a distinguished role that water vapor is playing in this one-layer model.

It is also noticed that by building up (or reducing) the atmospheric  $CO_2$  concentration, the disappearance of the snowball climate (or ice-free climate) will be induced. For example, based on this model, when  $A < 177W/m^2$ , which implies a very high  $CO_2$  concentration, the stable snowball climate will disappear; when  $A > 266W/m^2$ , which implies a very low  $CO_2$  concentration, the stable ice-free climate will disappear. Although these critical values might be too rough to make any certain conclusions, it presents a simple trend of climate states as the atmospheric  $CO_2$  concentration changes.

Therefore basically three steady states have been found in this one-layer diffusive moist static energy balance model, of which one represents a stable ice-free climate where temperature is relatively high everywhere and the temperature gradient is relatively small from the equator to the poles. The other one shows an unstable climate while the third one is a snowball climate. In addition, this model represents the possibility of abrupt climate transitions, for example, the transition from the snowball climate to the unstable climate state, or and the transition from the unstable climate state to the ice-free climate state when temperature gets higher due to increased atmospheric  $CO_2$  concentration, for example. Finally the model demonstrates one of the most important roles that water vapor is playing on the real climate, i.e. the meridional moisture energy transport that helps wipe

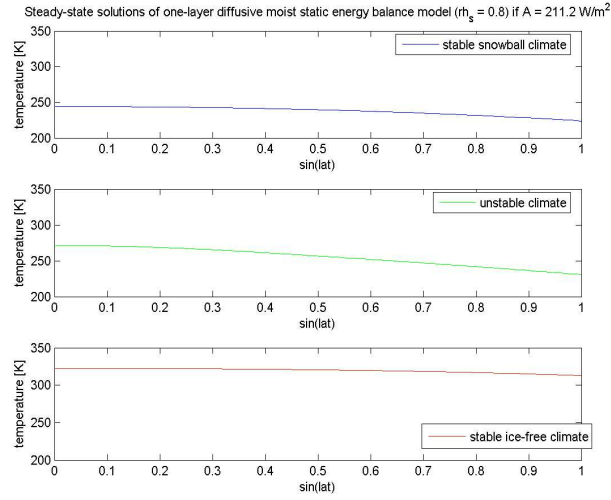


Figure 2: Steady-state solutions of one-layer diffusive moist static energy balance model if  $A = 211.2 \text{ W/m}^2$ . The top, middle and bottom panels present the global mean surface temperature in a stable snowball climate, an unstable climate which is  $20 \text{ K}$  lower than the current one, and a stable ice-free climate, respectively. Model parameters are the same as before.

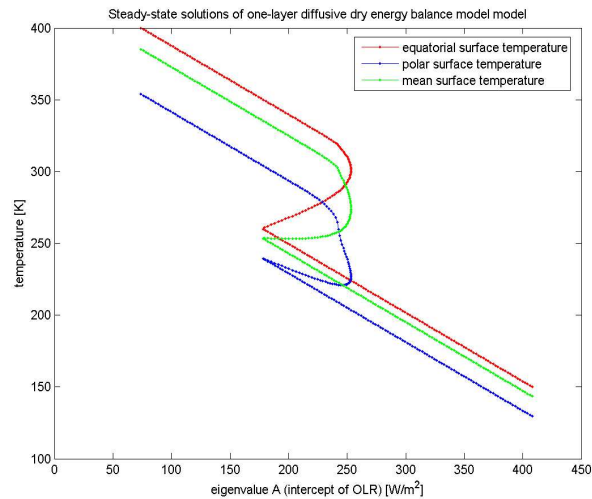


Figure 3: Steady-state solutions of one-layer diffusive dry energy balance model as a function of  $A$ . Same model parameters.

out the temperature gradient from the equator to the poles. However, the model has several limitations: one is that it cannot produce the current climate, either the temperature of the possible states is too high or too low. The second existing problem is that the effect of water vapor can not be much realized in this simple model.

Since this model is of one-layer, many important effects of water vapor can not be parameterized, such as the greenhouse effect, atmospheric convection and cloud cover. Hence we need to modify the model by adding some representation of cloud effects and hope for better outputs, such as the simulation of modern climate and so on.

## Two-Layer Model

### *a. Developing the Model*

An important effect of water vapor on the climate is the formation of clouds which have substantial interactions with both solar and terrestrial radiation. However, the impact of an individual cloud on the local energy balance depends sensitively on its physical characteristics, for example, the total mass of water, the size and shape of the droplets or particles and so on. Generally speaking, low-altitude stratus clouds have a large and negative cloud radiative forcing while high-altitude clouds are associated with a neutral or positive cloud radiative forcing. For my further discussion, I apply a simple representation of the greenhouse effect of clouds at first. As for the cloud albedo effect, it is closely related to the solar flux at certain latitude and time. The model should have seasonal cycle included then since, for example, at polar darkness, there is only greenhouse effect of clouds and it is discussed in Section 4.

Abbot and Tziperman (2007)[2] proposed an idea of convective cloud feedback to help explain the equable climate during the late Cretaceous and early Paleogene (about 100 million to 35 million years ago). At high latitudes under lower solar insolation, it is potentially possible to have a positive cloud radiative forcing with clouds associated with convection. If the extratropical surface temperature had increased large enough to initiate high convection, clouds would change from low-altitude to high-altitude ones and thus cloud radiative forcing would switch to positive from negative which could lead to further warming and even more atmospheric convection. Simulations done by Abbot and Tziperman[3][2] have shown that not only the high temperature situation at high latitudes and during winter time but also the relative low equator to pole temperature difference can be reproduced with the idea of high-latitude convective cloud feedback.

The model is composed of two layers[1]. The top one represents the free troposphere (200 – 900mb) and the bottom one represents the surface layer which is composed of the mixed-layer ocean (top 50m) and the boundary layer of the atmosphere (900 – 1000mb) dominated by turbulence. The energy balance of this model can be written as

$$C_s \frac{\partial T_s}{\partial t} = \frac{\partial}{\partial y} [(1 - y^2) D_1 \frac{\partial T_s}{\partial y}] + L_{\odot} (1 - \alpha) F(y) - F_c + \epsilon \sigma T_a^4 - \sigma T_s^4 \quad (11)$$

$$C_a \frac{\partial T_a}{\partial t} = \frac{\partial}{\partial y} [(1 - y^2) D_2 \frac{\partial T_a}{\partial y}] + F_c + \epsilon \sigma (T_s^4 - 2T_a^4) \quad (12)$$

where  $C_s$  and  $C_a$  are the thermal inertia for the bottom and top layer, respectively;  $T_s$  and  $T_a$  are the surface and atmospheric temperature, respectively;  $D_1$  and  $D_2$  are the diffusive

coefficients for the bottom and top layer, respectively (the two diffusive coefficients should be different in principle but are assumed to be the same at first); the first terms on the right hand side of the equations are the diffusive heat transport at the bottom and top layers, respectively;  $F_c$  is the convective flux from the boundary layer to the free troposphere;  $\epsilon$  is the emissivity of the free troposphere; and  $\sigma$  is the Stefan-Boltzmann constant. Boundary conditions of this two-layer model are similar to that of the one-layer model, i.e.

$$\frac{dT_s}{dy}(y=0) = \frac{dT_a}{dy}(y=0) = 0 \quad (13)$$

$$T_s(y=1) \text{ and } T_a(y=1) \text{ are regular.} \quad (14)$$

The value of convective flux  $F_c$  and emissivity  $\epsilon$  depends on whether there is convection or not, which is in turn described by moist instability. We determine the moist instability by comparing the surface moist static energy

$$M_s = C_p T_s + L_v q_s \quad (15)$$

with the atmospheric saturation moist static energy

$$M_a^* = C_p T_a + L_v q_a^* + g z_a \quad (16)$$

where  $q_a^*$  is the atmospheric saturation specific humidity,  $g$  is the acceleration of gravity,  $z_a$  and  $p_a$  are the height and pressure of the atmospheric layer, respectively. The convective flux  $F_c$  and emissivity  $\epsilon$  are given by

$$F_c = \begin{cases} \gamma(M_s - M_a^*) & \text{if } M_s \geq M_a^* \\ 0 & \text{otherwise} \end{cases} \quad (17)$$

$$\epsilon = \begin{cases} \epsilon_o + \Delta\epsilon & \text{if } M_s \geq M_a^* \\ \epsilon_o & \text{otherwise} \end{cases} \quad (18)$$

If  $M_s < M_a^*$ , ascending parcel is stable to moist convection and thus no convection happens. In this nonconvecting case,  $F_c$  is set to be 0 and atmospheric emissivity  $\epsilon$  is given by the background emissivity  $\epsilon_o$  which is mainly determined by the atmospheric  $CO_2$  concentration and is roughly linear in  $\log(CO_2)$  (Sasamori, 1968 [10]). As long as the moist static energy of the ascending parcel reaches the atmospheric saturation moist static energy, i.e.  $M_s = M_a^*$ , the parcel becomes unstable to convection and releases latent heat to the surrounding environment, and thus  $F_c$  is set to be linear of  $M_s - M_a^*$  with a linear coefficient  $\gamma$  given by  $\frac{C_s}{C_p} \frac{1}{\tau}$ , where  $\tau$  is the time scale of convection, for example, about 1 – 10 hours, and atmospheric emissivity is increased by a certain amount  $\Delta\epsilon$  due to convective clouds and increased atmospheric moisture.

### *b. Equilibria in the Model*

The two joint nonlinear ODEs (steady state of equations 11 and 12) are solved numerically to find out the solutions of steady-state surface and atmospheric temperature. For the same background emissivity  $\epsilon_o$ , steady-state solutions are sensitive to the initial guesses and thus there again exists bifurcation in the solutions. Same as the numerical method



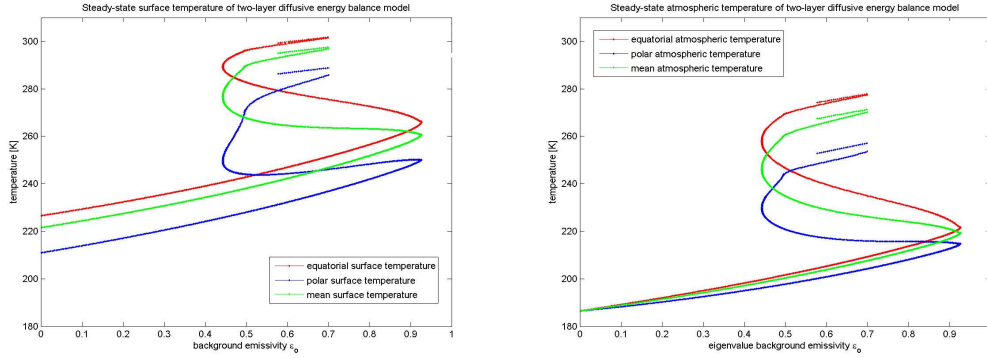


Figure 4: Steady-state surface temperature (left) and atmospheric temperature (right) of two-layer diffusive moist static energy balance model as a function of background emissivity  $\epsilon_o$ , which is roughly linear in  $\log(CO_2)$  concentration. Part of the convecting branch where the total atmospheric emissivity  $\epsilon$  is larger than 1 is not physical and not shown here. Model parameters are:  $\Delta\epsilon = 0.3$ ,  $\gamma = 5.8101kg/m^2/s$ ,  $RH_s = 0.8$ ,  $z_a = 5km$ ,  $\alpha_i = 0.6$ ,  $\alpha_o = 0.1$ ,  $T_i = 260K$ ,  $T_o = 290K$ .

in one-layer model, we solve the background emissivity  $\epsilon_o$  as an unknown eigenvalue by prescribing the equatorial surface temperature. Figure 4 shows the bifurcation diagrams of the steady-state surface and atmospheric temperature produced by the two-layer model. In particular,  $\Delta\epsilon$  is set to be 0.3, and thus part of the bifurcation diagram where the total atmospheric emissivity  $\epsilon$  is larger than 1 (or the background emissivity  $\epsilon_o$  is larger than 0.7) has no physical meaning and is not drawn here since  $0 \leq \epsilon \leq 1$ . If it starts with a background emissivity larger than 0.7 and has convection happening, then the steady-state solution will stay with the atmospheric emissivity equals 1.

One of the interesting features of the bifurcation diagram of this model is that there are two more equilibrium solutions around  $\epsilon_o = 0.6$  and when surface temperature is relatively high. Physical interpretation of the solutions in the following demonstrates that one is a stable equilibrium corresponding to a fully convecting state where surface temperature is high and convection happens everywhere from the equator to the poles, and the other one is an unstable equilibrium which is not shown in the figures. The problem with the unstable equilibrium branch (not shown) is that it is hard to find the solution numerically with the method other steady-state solutions are figured out. By doing projection onto Legendre polynomials and characterizing the steady-state solutions by first few modes, the unstable equilibrium branch can be found numerically but without high accuracy. Since the numerical computation is not reliable so far, it is not shown here.

In order to further understand the physics of the bifurcation diagram, a diagnosis of temperature and convection situation has been done in the following for various steady states, for example, states  $\langle 1 \rangle - \langle 11 \rangle$  marked in Figure 5. Figure 6, 7, 8, 9 show the steady-state atmospheric and surface temperature, i.e.  $T_a$  and  $T_s$ , and  $\Delta M = M_s - M_a^*$  which is a measure of whether there is convection or not as a function of  $y$  for these 11 states, respectively. If the surface temperature is very low, there is no possibility of convection where the moist instability is negative everywhere from the equator to the poles.

It is the same stable snowball climate as represented in one-layer model (states  $\langle 1 \rangle$   $\langle 2 \rangle$   $\langle 3 \rangle$  shown in Figure 6). If the equatorial surface temperature increases and reaches some critical value such that  $M_s = M_a^*$ , moist convection will firstly take place at the equator. The transition of convection at the equator corresponds to the first edge in the bifurcation diagram. As the equatorial surface temperature gets higher and higher, the upper atmospheric layer becomes moist unstable and convection can be initiated gradually from latitude to latitude. As shown in Figure 7 and 8, moist convection extends from the equator to the poles as the equatorial surface temperature increases, but since up to, for example, state  $\langle 8 \rangle$ , convection doesn't come out at the poles yet, we name it partially convecting state. However, stability analysis tells that the branch where states  $\langle 4 \rangle$  and  $\langle 5 \rangle$  (in Figure 7) lie is unstable while the one which has states  $\langle 6 \rangle$ ,  $\langle 7 \rangle$ ,  $\langle 8 \rangle$  (in Figure 8) is stable, and this transition corresponds to the second edge of the bifurcation diagram. This is also consistent with the stability results in one-layer model. Eventually moist convection occurs at the poles when the surface equatorial temperature is large enough and this is what Figure 9 shows in which moist instability is positive at the poles. Due to the fact that convection takes place everywhere from the equator to the poles in states  $\langle 9 \rangle$ ,  $\langle 10 \rangle$ ,  $\langle 11 \rangle$ , we name them fully convecting states. Although the unstable missing branch is hard to compute numerically, it is related to the transition of polar convection when the moist instability of state  $\langle 8 \rangle$  is compared with that of state  $\langle 9 \rangle$ . The stability of each branch can also be checked by identifying the eigenvalues of the Jacobian matrix estimated at equilibrium states in perturbation equation. Therefore in conclusion the bifurcation diagram of the two-layer model is composed of several steady-state branches, for example, a stable nonconvecting branch, an unstable partially convecting branch, a stable partially convecting branch, an unstable branch which is related to the onset of polar convection, and a stable fully convecting branch.

Moreover the stable partially convecting state where the background emissivity  $\epsilon_o = 0.46$  roughly represents the modern climate with  $293K$  at the equator and  $257K$  at the poles. It demonstrates that the implement of convective cloud feedback helps better simulate the real climate and the impact of clouds is significant on climate.

### *c. Climate Sensitivity in the Model*

There are several free parameters in the two-layer model, such as surface relative humidity  $RH_s$ , height of the atmospheric layer  $z_a$  and linear coefficient of convective flux  $\gamma$ . Our next step is to study the climate sensitivity of this model by varying these free parameters. Climate sensitivity is a significant component and is defined as the relationship between the forcing and the magnitude of the climate change response. The study of climate sensitivity can help better understand and interpret the model and also the physics of it.

As the surface relative humidity increases, the parcel lifted upward from the surface can get saturated more easily and thus convection can be initiated more quickly. With a high surface relative humidity convection can occur early before the surface temperature there reaches a high value. The numerical comparison of the bifurcation diagrams of different surface relative humidity is shown in Figure 10. Figure 11 represents the steady-state solutions of different heights of atmospheric layer. For the climate sensitivity of the height of the atmospheric layer, as the height decreases, the onset of convection can be more easily

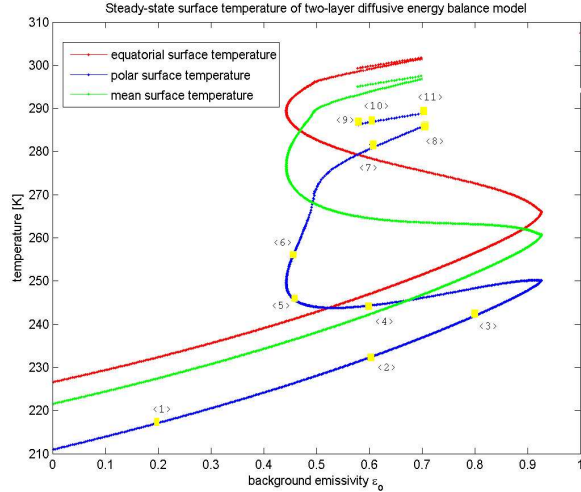


Figure 5: Steady-state surface temperature of two-layer diffusive moist static energy balance model as a function of background emissivity  $\epsilon_o$  which is roughly linear in  $\log(CO_2)$  concentration. Various steady-state solutions, for example, states  $\langle 1 \rangle - \langle 11 \rangle$  are marked.

initiated at each latitude and the transition to both partially and fully convecting branches can be reached with a lower surface temperature compared with the case of a higher atmospheric layer. Figure 12 represents the steady-state solutions of different linear coefficients of convective flux. The linear coefficient of convective flux  $\gamma$  determines the magnitude of convective flux transferred from the boundary layer to the free troposphere when convection happens. Since the time scale of convection can vary within 1 – 10 hours, small changes of  $\gamma$  in this model are physically reasonable. As  $\gamma$  gets smaller, the top atmospheric layer gets less convective flux from the bottom one, which reduces the saturation moist static energy in the atmospheric layer. In this case, convection again can be more easily initiated which leads to the situation of fully convection at a lower surface temperature compared with the case with larger  $\gamma$ . The difference between this case and the former two is that varying the value of  $\gamma$  only changes the critical surface temperature of the onset of moist convection but keeps the structure (relationship between background emissivity and surface temperature) of convecting branches, i.e. both partially convecting and fully convecting branches, invariant. My understanding is that the structure of convecting branches is merely determined by  $M_s = M_a^*$  and  $\gamma$  has nothing to do with this criterion, which is different from the former two cases of varying  $RH_s$  and  $z_a$ .

#### d. Seasonal Cycle in the Model

In addition to convective cloud feedback, cloud albedo effect is also included into the two-layer model. Since cloud albedo effect is closely related to the solar incoming radiation at top of the atmosphere, the two-layer model should also have the seasonal variability since, for example, at polar darkness, there is no solar radiation, and the only effect of clouds is

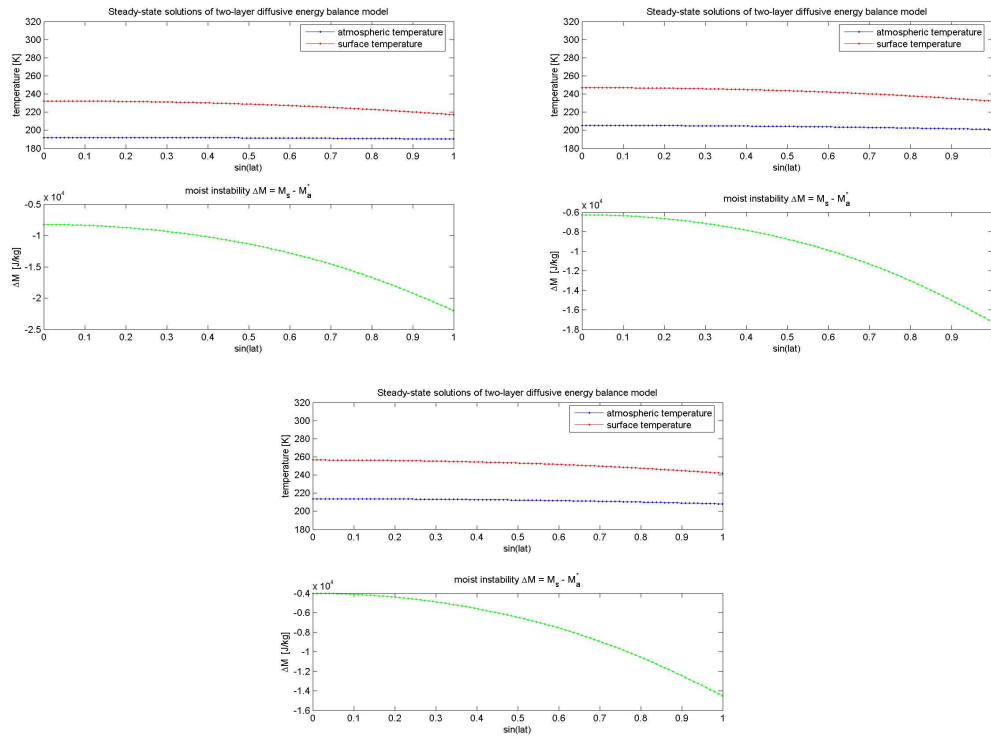


Figure 6: Steady-state surface temperature, atmospheric temperature, and moist instability measured by  $\Delta M = M_s - M_a^*$  at equilibrium states  $\langle 1 \rangle$  (top left),  $\langle 2 \rangle$  (top right) and  $\langle 3 \rangle$  (bottom) with corresponding background emissivity  $\epsilon_o = 0.2, 0.6, 0.8$ , respectively. Nonconvecting. Stable.

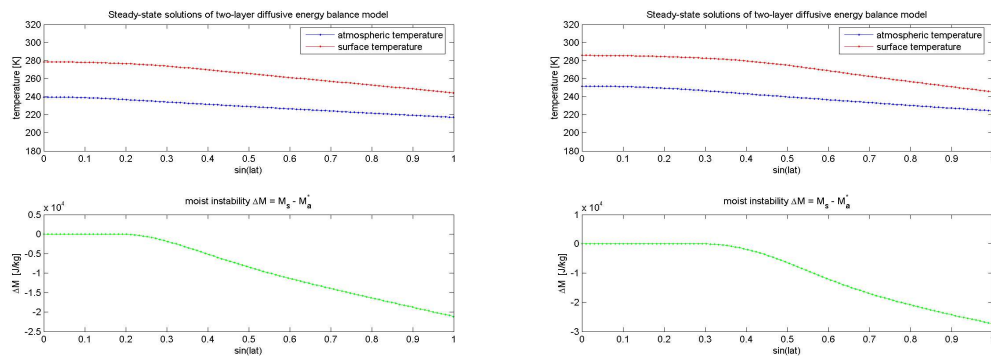


Figure 7: Steady-state surface temperature, atmospheric temperature, and moist instability measured by  $\Delta M = M_s - M_a^*$  at equilibrium states  $\langle 4 \rangle$  (left) and  $\langle 5 \rangle$  (right) with corresponding background emissivity  $\epsilon_o = 0.6, 0.46$ , respectively. Partially convecting (Convection firstly takes place in tropics and extends to high latitudes, but doesn't come out at the poles yet). Unstable.

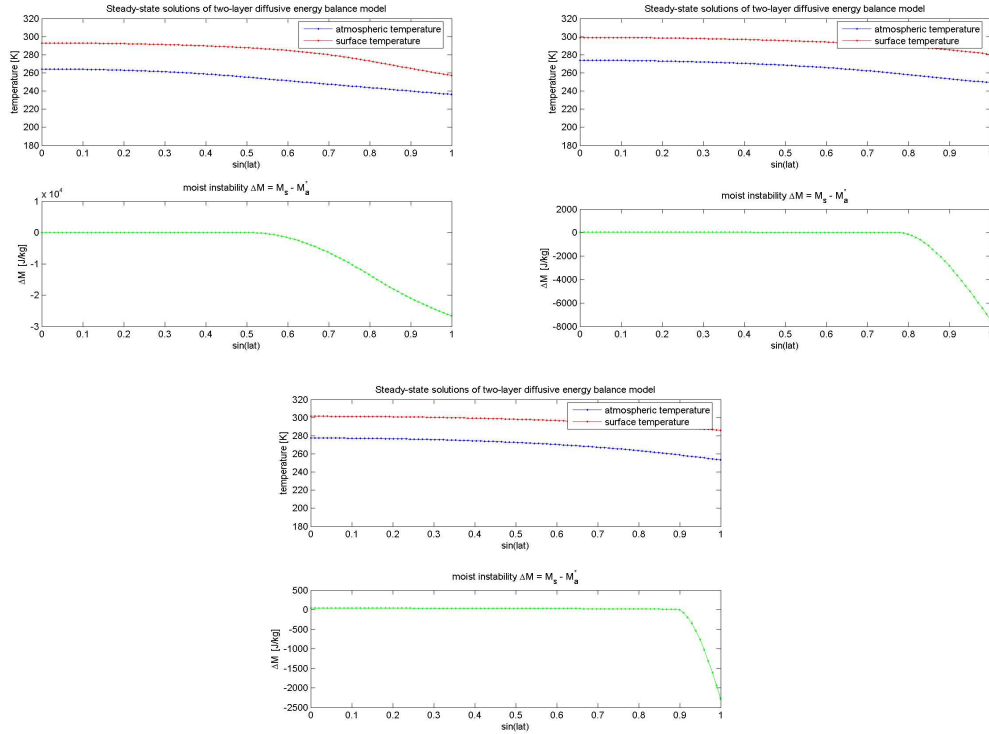


Figure 8: Steady-state surface temperature, atmospheric temperature, and moist instability measured by  $\Delta M = M_s - M_a^*$  at equilibrium states < 6 >(top left), < 7 >(top right) and < 8 >(bottom) with corresponding background emissivity  $\epsilon_o = 0.46, 0.6, 0.7$ , respectively. Partially convecting. Stable. State < 6 > whose background emissivity  $\epsilon_o = 0.46$  roughly represents the modern climate with  $293K$  at the equator and  $257K$  at the poles.

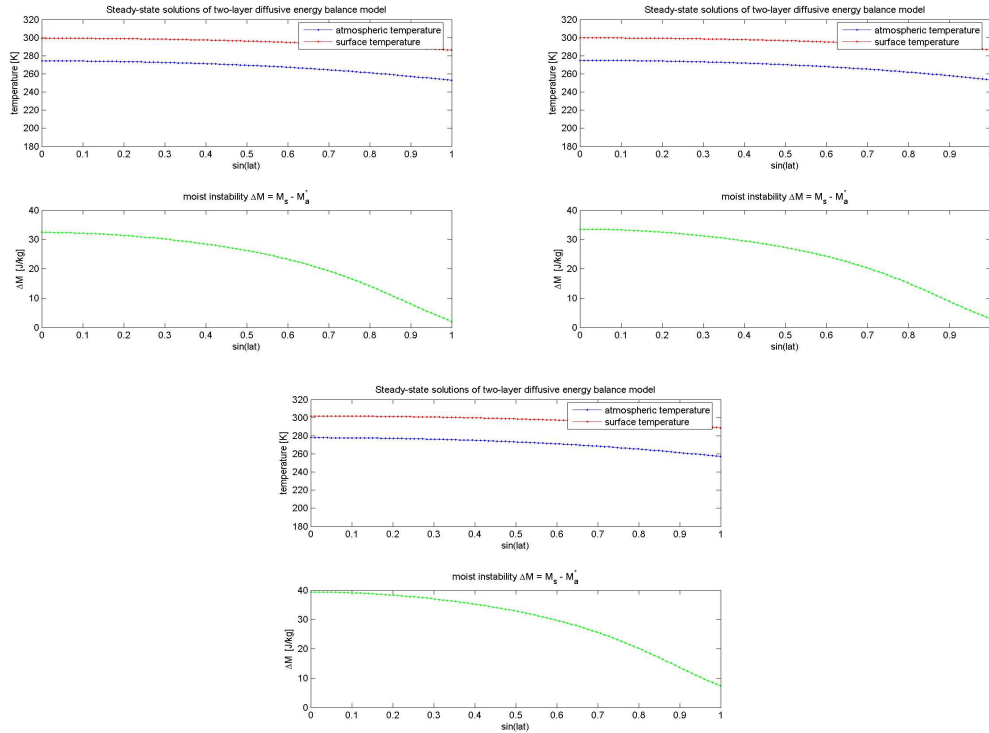


Figure 9: Steady-state surface temperature, atmospheric temperature, and moist instability measured by  $\Delta M = M_s - M_a^*$  at equilibrium states  $\langle 9 \rangle$  (top left),  $\langle 10 \rangle$  (top right) and  $\langle 11 \rangle$  (bottom) with corresponding background emissivity  $\epsilon_o = 0.58, 0.6, 0.7$ , respectively. Fully convecting (Convection takes place everywhere from the equator to the poles). Stable.

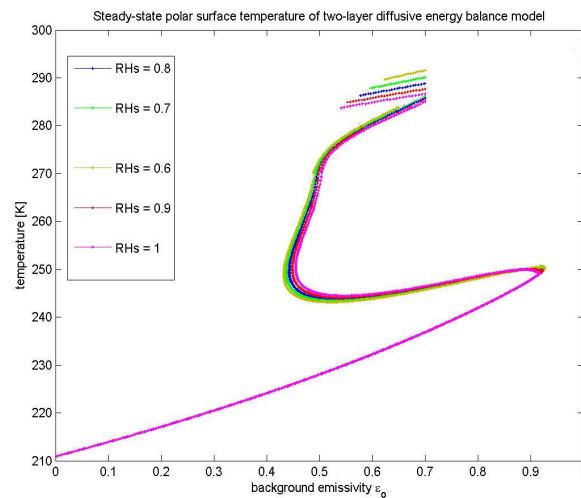


Figure 10: Steady-state polar surface temperature of two-layer diffusive energy balance model with surface relative humidity  $RH_s = 0.6, 0.7, 0.8, 0.9, 1$ , respectively.

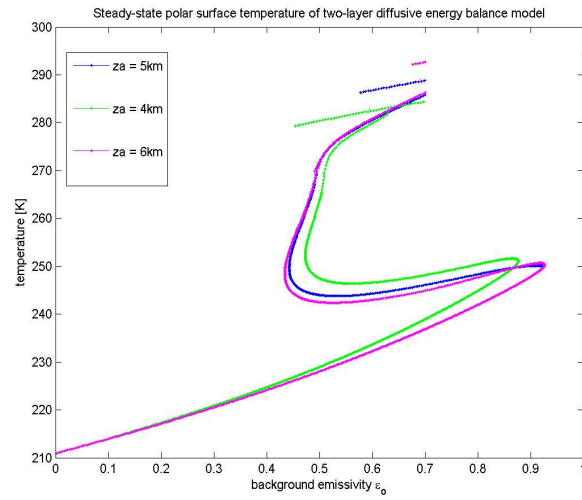


Figure 11: Steady-state polar surface temperature of two-layer diffusive energy balance model with height of the atmospheric layer  $z_a = 4\text{km}, 5\text{km}, 6\text{km}$ , respectively.

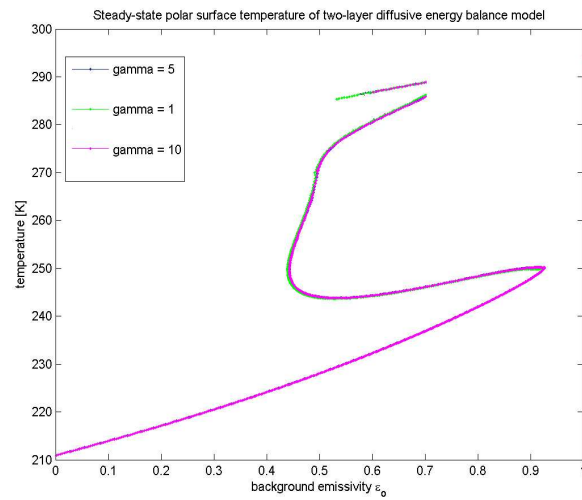


Figure 12: Steady-state polar surface temperature of two-layer diffusive energy balance model with  $\gamma = 1\text{kg/m}^2/\text{s}, 5\text{kg/m}^2/\text{s}, 10\text{kg/m}^2/\text{s}$ , respectively.

the albedo effect.

In order to figure out the average daily insolation[6] at top of the atmosphere as a function of time and latitude, some parameters are introduced beforehand. First of all, solar zenith angle  $\theta_s$  is defined as the angle between the local normal to Earth's surface and the direction of incoming solar flux and determines the actual solar flux per unit surface area  $Q$ , which is given by

$$Q = L_{\odot} \left(\frac{\bar{d}}{d}\right)^2 \cos\theta_s \quad (19)$$

where  $\bar{d}$  is the mean distance from the sun where the solar constant is measured and  $d$  is the actual distance. There is less energy per unit surface area if the surface is not perpendicular to the incoming solar flux compared with that in the perpendicular case. Secondly, declination angle  $\delta$ , which is defined as the latitude of the point on the surface of Earth directly under the sun at noon, varies between  $+23.45^\circ$  at northern summer solstice (June 21) and  $-23.45^\circ$  at northern winter solstice (December 21). Finally the longitude of the subsolar point relative to its position at noon is defined as the hour angle  $h$ . The relationship between the above three parameters, i.e. solar zenith angle  $\theta_s$ , declination angle  $\delta$ , hour angle  $h$ , and the latitude  $\phi$  is given by

$$\cos\theta_s = \sin\phi\sin\delta + \cos\phi\cos\delta\cos h. \quad (20)$$

When it is sunrise or sunset,  $\cos\theta_s = 0$ , and the hour angle of sunrise and sunset is given by

$$\cos h_o = -\tan\phi\tan\delta. \quad (21)$$

Then if we plug (20) into (19) and integrate it from sunrise to sunset, the average daily insolation at top of the atmosphere can be rewritten as

$$\bar{Q}^{\text{day}} = \frac{L_{\odot}}{\pi} \left(\frac{\bar{d}}{d}\right)^2 [h_o \sin\phi\sin\delta + \cos\phi\cos\delta\sin h_o]. \quad (22)$$

However there are special conditions at the poles. When the latitude  $\phi$  and the declination angle  $\delta$  are of the same sign, which is the case in summer hemisphere, latitudes poleward of  $90 - \delta$  are constantly illuminated. In addition, when the latitude  $\phi$  and the declination angle  $\delta$  are of the opposite sign, which is the case in winter hemisphere, latitudes poleward of  $90 - |\delta|$  are in polar darkness. Therefore, at polar region, six months of darkness alternates with six months of sunlight. Hence the governing equations become two joint nonlinear PDEs given by

$$C_s \frac{\partial T_s}{\partial t} = \frac{\partial}{\partial y} [(1 - y^2) D_1 \frac{\partial T_s}{\partial y}] + \bar{Q}^{\text{day}} (1 - \alpha) - F_c + \epsilon \sigma T_a^4 - \sigma T_s^4 \quad (23)$$

$$C_a \frac{\partial T_a}{\partial t} = \frac{\partial}{\partial y} [(1 - y^2) D_2 \frac{\partial T_a}{\partial y}] + F_c + \epsilon \sigma (T_s^4 - 2T_a^4). \quad (24)$$

Since solar flux is not symmetric between the two hemispheres in this time-dependent case, the seasonal model and its solutions are not symmetric anymore. The condition of  $T_s(y = \pm 1)$  and  $T_a(y = \pm 1)$  are regular gives the boundary condition. If there is convection within some region, not only convective flux  $F_c$  and atmospheric emissivity  $\epsilon$  as mentioned



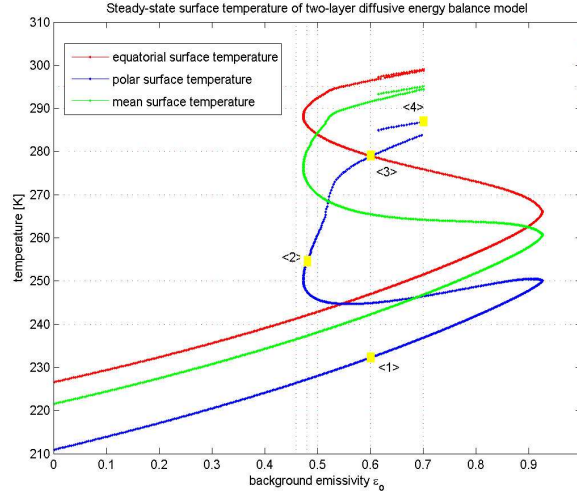


Figure 13: Steady-state surface temperature of two-layer diffusive energy balance model when cloud albedo effect is taken into account but without seasonal cycle at first. If convection takes place within some region, albedo there is assumed to increase by 0.05 in the simulation.

before, but also albedo within that region will change, for example, albedo will increase by 0.05 due to clouds' reflection of solar incoming radiation. The corresponding bifurcation diagram of steady-state solutions is represented in Figure 13 in which cloud albedo effect is taken into account but without seasonal cycle at first. It shows that due to the effect of cloud albedo, the bifurcation diagram is shifted to the right compared with Figure 5.

The above two joint nonlinear PDEs can be solved numerically and the time-dependent solutions of different initial guesses, for example, states 1 – 4 in Figure 13, are represented in Figure 14 – 17. The solutions of surface temperature at South Pole, at North Pole and at the equator are plotted every 12 months. When running the seasonal model with initial guess of state < 1 > which is a stable nonconvecting state, the time-dependent solution is wild at the beginning but eventually reaches a periodic equilibrium after about 1500 months, which is shown in Figure 14. In Figure 15, if the seasonal model starts with initial guess of state < 2 >, a stable partially convecting state, the solution quickly jumps to the snowball climate within a short time period. As shown in Figure 16, the time-dependent solution periodically oscillates around the initial steady-state equilibrium, i.e. the stable partially convecting state < 3 >. In Figure 17 which is the time-dependent solution with initial guess of state < 4 >, it is roughly periodic but with several abrupt sharp transitions. Since these abrupt transitions are transient, the intermediate states are unstable. It is interesting to notice that state < 4 > is a stable fully convecting state and is very close to the unstable missing branch that we mentioned before. It is reasonable to explain the existence of these abrupt transient transitions in this way: oscillations around the initial steady-state equilibrium < 4 > allow the possibility of transition to lower unstable branch, however, the time-dependent solution has to find other stable states such as the stable partially convecting states and the stable fully convecting states due to the instability of

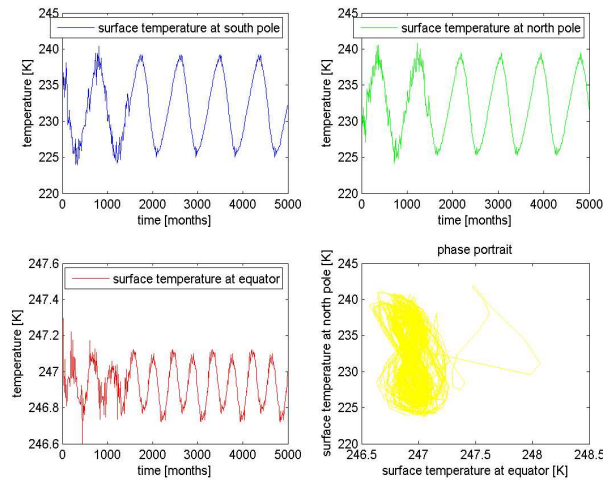


Figure 14: Time-dependent solution of the seasonal model with an initial guess of state  $\langle 1 \rangle$  in Figure 13, i.e.  $233K$  at the poles and  $247K$  at the equator and with background emissivity  $\epsilon_o = 0.6$ . Time is in the unit of month. The top left panel is the surface temperature at south pole as a function of time, the top right one is the surface temperature at north pole as a function of time, the bottom left one is the surface temperature at the equator as a function of time, and the bottom right one is the phase portrait with x-axis the surface temperature at the equator and y-axis the surface temperature at north pole.

the lower branch. It is another indirect indicator of the existence of the unstable branch that is related to the transition of polar convection.

## Conclusions

We start the problem trying to figure out the effect of water vapor in the climate system in simplified model simulations. A one-layer diffusive moist static energy balance model is applied at first. From the model output, three possible steady climate states, i.e. a stable snowball climate, an unstable climate in which surface temperature is about  $20K$  lower than the modern value everywhere, and a stable ice-free climate, have been found, moreover, the effect of water vapor is represented mainly by the meridional moisture transport to the poles through the comparison with dry model. However, even if all the model parameters are based on modern climate observations, the one-layer model is unable to produce the modern climate. In order to better simulate the real climate, a two-layer diffusive energy balance model has been developed in which an important effect of water vapor, i.e. convective cloud feedback, is parameterized through the impact of convective flux and atmospheric emissivity. The solutions of this model are very interesting. First of all, it is able to roughly represent the modern climate which in turn indicates the significance of clouds effect in real climate. Furthermore, two more steady equilibrium states, besides the three equilibria turned out in one-layer model, have been found due to the implement of convective cloud feedback. Significantly, each equilibrium has its clear physical meaning. For example, when

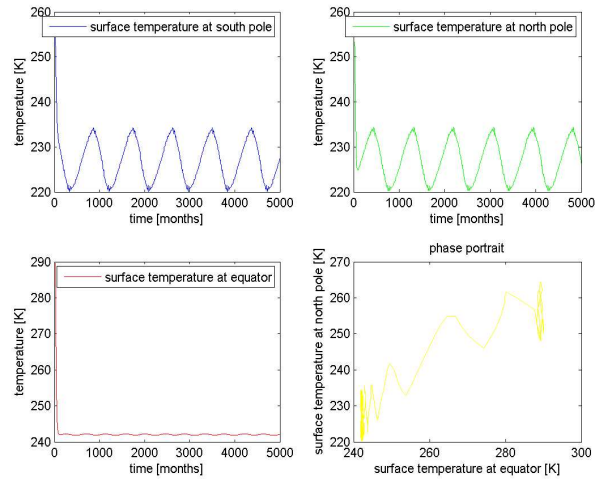


Figure 15: Time-dependent solution of the seasonal model with an initial guess of state  $\langle 2 \rangle$  in Figure 13, i.e.  $254K$  at the poles and  $290K$  at the equator and with background emissivity  $\epsilon_o = 0.48$ . Time is in the unit of month. Others are the same as Figure 14.

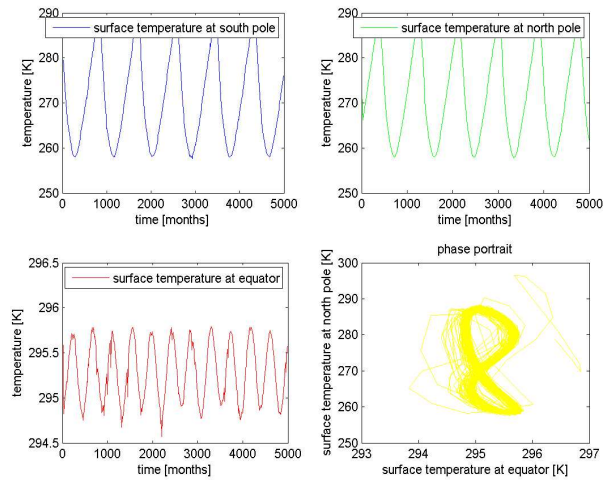


Figure 16: Time-dependent solution of the seasonal model with an initial start of state  $\langle 3 \rangle$  in Figure 13, i.e.  $279K$  at the poles and  $296K$  at the equator and with background emissivity  $\epsilon_o = 0.6$ . Time is in the unit of month. Others are the same as Figure 14.

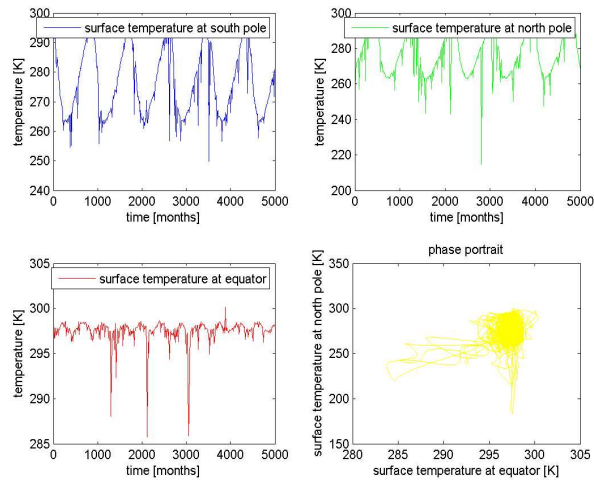


Figure 17: Time-dependent solution of the seasonal model with an initial start of state  $\langle 4 \rangle$  in Figure 13, i.e.  $287K$  at the poles and  $299K$  at the equator and background emissivity  $\epsilon_o = 0.7$ . Time is in the unit of month. Others are the same as Figure 14.

surface temperature is very low everywhere, there is no possibility of convection because it is always moist stable, and it is the same equilibrium state that is noticed in one-layer model. As the equatorial surface temperature reaches some critical value, convection takes place at the equator firstly. As the equatorial surface temperature gets higher, convection takes place at high latitudes. Eventually there is convection at the poles when temperature is relatively high. One of the two more equilibria in two-layer model represents a stable climate state with convection taking place everywhere from the equator to the poles while the other one is an unstable branch that is related to the transition of polar convection. The last section of the project is the seasonal model, in which both the seasonal cycle of solar insolation and cloud albedo effect are included. The time-dependent solutions are basically oscillations around steady equilibria of constant solar insolation. Depending on how large the variability of climate is at each state, it is possible to switch from one equilibrium to another, for example, the transition to snowball climate from a warmer climate state.

Although this study is basically based on a simple two-layer energy balance model, it is able to capture the basic but essential physics of convective cloud feedback and produce multiple steady equilibria in addition to temperature distribution of modern climate. Since the model is a simplified version, the physics can be understood completely and clearly. Furthermore, it indicates the importance of convective cloud feedback of real climate. However, since the model is simply parameterized and only includes few effects and feedbacks in real climate, the results from the model cannot be simply compared with real climate situation. For example, albedo is a complicated variable which not only depends sensitively on the surface and clouds situation but also varies with time and has feedback to the climate, and the real effect of clouds is much more complicated than what is parameterized in the model. More numerical computation and analysis will be done on the seasonal model and its time-dependent solutions in the future.

## Acknowledgements

Great thanks to Neil Balmforth, who helped me throughout the whole summer about the project, Eli Tziperman, who gave me helpful suggestions on the improvement of models and physical interpretation, and Raymond Pierrehumbert, who brought up this interesting project. Also many thanks to Joseph Keller and Dorian Abbot for helpful discussions. Final thanks to the Geophysical Fluid Dynamics summer program and all the faculty and fellows.

## References

- [1] D. S. ABBOT AND E. TZIPERMAN, *Controls on the activation and strength of a high latitude convective cloud feedback*, J. Atmos. Sci., (2008).
- [2] ———, *A high latitude convective cloud feedback and equable climates*, Quart. J. Roy. Meteor. Soc., 134 (2008), pp. 165–185.
- [3] ———, *Sea ice, high latitude convection, and equable climates*, Geophys. Res. Lett., 35 (2008), pp. L03702, doi:10.1029/2007GL032286.
- [4] M. I. BUDYKO, *The effect of solar radiation variations on the climate of the earth*, Tellus, 21 (1969), pp. 611–619.
- [5] P. Z.-G. DARGAN M. W. FRIERSON, ISAAC M. HELD, *A gray-radiation aquaplanet moist gcm. part 2: Energy transports in altered climates*, J. Atmos. Sci., 64 (2006), pp. 1680–1693.
- [6] D. L. HARTMANN, *Global Physical Climatology*, Academic Press, 1994.
- [7] IPCC, *Climate Change 2007, Synthesis Report to the fourth assessment of the Intergovernmental Panel on Climate Change*, Intergovernmental Panel on Climate Change, 2007.
- [8] G. R. NORTH, *Theory of energy-balance climate models*, J. Atmos. Sci., 32 (1975), pp. 2033–3043.
- [9] G. R. NORTH, R. F. CAHALAN, AND J. JAMES A. COAKLEY, *Energy balance climate models*, Reviews of Geophysics and Space Physics, 19 (1981), pp. 91–121.
- [10] T. SASAMORI, *The radiative cooling calculation for application to general circulation experiments*, J. Appl. Meteor., 7 (1968), pp. 721–729.
- [11] W. D. SELLERS, *A climate model based on the energy balance of the earth-atmosphere system*, J. Appl. Meteor., 8 (1969), pp. 392–400.